

STARS

University of Central Florida
STARS

Honors Undergraduate Theses

UCF Theses and Dissertations

2019

Stochasticity in an Artificial Neuron using Ag/2D-MoS₂/Au Threshold Switching Memristor

Madison Manley
University of Central Florida

Find similar works at: <https://stars.library.ucf.edu/honorsthesis>
University of Central Florida Libraries <http://library.ucf.edu>

Recommended Citation

Manley, Madison, "Stochasticity in an Artificial Neuron using Ag/2D-MoS₂/Au Threshold Switching Memristor" (2019). *Honors Undergraduate Theses*. 645.
<https://stars.library.ucf.edu/honorsthesis/645>

This Open Access is brought to you for free and open access by the UCF Theses and Dissertations at STARS. It has been accepted for inclusion in Honors Undergraduate Theses by an authorized administrator of STARS. For more information, please contact lee.dotson@ucf.edu.



STOCHASTICITY IN AN ARTIFICIAL NEURON USING AG/2D-MOS₂/Au
THRESHOLD SWITCHING MEMRISTOR

by

MADISON MANLEY

A thesis submitted in partial fulfilment of the requirements
for the Honors in the Major Program in Electrical Engineering
in the College of Engineering
and in the Burnett Honors College
at the University of Central Florida
Orlando, Florida

Thesis Chair: Dr. Tania Roy

ABSTRACT

Neuromorphic computing comprises of systems that are based on the human brain or artificial neural networks, with the promise of creating a brain inspired ability to learn and adapt, but technical challenges, such as developing an accurate neuroscience model of the functionality of the brain to building devices to support these models, are significantly hindering the progress of neuromorphic systems. This has paved the way for artificial neural networks (ANN) to meet these criteria. The memristor has become an emerging candidate to realize ANN through emulation synapse and neuron behavior. In this work, we are fabricating an Ag/MoS₂/Au threshold switching memristor (TSM), to emulate four critical behaviors of neurons - all-or-nothing spiking, threshold-driven firing, post firing refractory period and stimulus strength-based frequency response. We will also test the innate stochastic behavior of these devices to see if they are voltage dependent, making them a possible application in the integrate and fire neuron. Continuing to emulate biological synapses using memristors can help solve many optimization and machine learning problems, which in turn, can make electronics as energy-efficient as our brain.

ACKNOWLEDGEMENTS

I'd first like to thank my research advisor Dr. Tania Roy for her support and guidance throughout my undergraduate career at the University of Central Florida. She has provided me with invaluable advice and feedback to help me become a better researcher in all aspects and I am incredibly thankful for all that she has taught me these past four years. I would also like to thank Dr. Jiann Yuan for being on my thesis committee and for reading this thesis report.

Finally, I would like to thank everyone in the Roy lab at UCF. Thank you to Molla Manjurul Islam and Ricardo Martinez for their support throughout this process. I would like to thank Dr. Sonali Das for helping me improve this report and helping me prepare my defense. I would especially like to thank Adithi Krishnaprasad and Durjoy Dev who fabricated the devices used in this project and for teaching me how to use the RT probe station to complete these electrical tests. Their help and guidance have made this possible.

TABLE OF CONTENTS

Part 1: Introduction	6
1.1 Neuromorphic Computing	6
1.2 Biological Neuron	7
1.2.1 Neuron Critical Behaviors	8
1.3 Threshold Switching Memristor (TSM).....	10
1.3.1 Previous Work Emulating Neuron Behavior	11
1.4 Innate Stochasticity	12
1.4.1 Modeling Stochastic Memristors	13
Part 2: Methodology	15
2.1 Device Structure.....	15
2.2 Artificial Neuron Spiking.....	16
2.3 Stochastic Measurements	17
Part 3: Results	19
3.1 Emulating Neuron Behavior	19
3.2 Statistics of Device Spiking Behavior.....	21
Part 4: Conclusion	24
References	25

LIST OF FIGURES

FIGURE 1: REPRESENTATION OF BIOLOGICAL NEURON [5].....	7
FIGURE 2: FEATURES OF ACTION POTENTIAL IN BIOLOGICAL NEURONS [6].....	8
FIGURE 3: SIMPLIFIED SCHEMATIC OF OUTPUT SPIKING OF NEURON WITH RESPECT TO THE INPUT THRESHOLD [5].....	9
FIGURE 4: OUTPUT SPIKE OF ARTIFICIAL NEURON SHOWING THE REFRACTORY AND INTEGRATION PERIOD OF THE NEURON [5].	9
FIGURE 5: STIMULUS STRENGTH-BASED FREQUENCY RESPONSE FOR V-MoS ₂ /GRAPHENE TSM. (A) (TOP) INPUT VOLTAGE PULSES OF AMPLITUDE 7.5V. (BOTTOM) TWO OUTPUT SPIKE OBSERVED FOR INPUT VOLTAGE PULSES OF AMPLITUDE 5V. (B) (TOP) INPUT VOLTAGE PULSES OF AMPLITUDE 5.2 V. (BOTTOM) THREE OUTPUT SPIKES OBSERVED FOR INPUT VOLTAGE PULSES OF AMPLITUDE 5.2 V [5].	10
FIGURE 6: CONCEPTUAL REPRESENTATION OF THE TSM BASED ARTIFICIAL NEURON [5].....	10
FIGURE 7: I-V CHARACTERISTICS OF AN Ag/SiO ₂ /Au TSM DEVICE [7].....	11
FIGURE 8: (A) THE TSM NEURON SPIKES UNDER DIFFERENT INPUT INTENSITIES. (B) STATISTICAL VOLTAGE/SPIKE-FREQUENCY RELATIONSHIP OF THE NEURON. (C) THE STATISTICAL PULSE NUMBER/AMPLITUDE RELATIONSHIP OF THE NEURON [7].	12
FIGURE 9: (A) SEM IMAGE OF A TiO ₂ MEMRISTOR CROSS-SECTION. (B) ILLUSTRATION OF A SIMPLE BARRIER MEMRISTOR MODEL. (C) FILAMENT FORMATION PROCESS IN A THIN-FILM [8].....	13
FIGURE 10: HISTOGRAMS OF THE WAIT TIME FOR THE FIRST SWITCHING EVENT OF Ag/A-Si/P-Si PILLAR STRUCTURE AT BIAS VOLTAGES 2.6, 3.2, AND 3.6 V, RESPECTIVELY [10].	14
FIGURE 11: STRUCTURE OF Ag/MoS ₂ /Au MEMRISTOR.....	15
FIGURE 12: OPTICAL IMAGE OF Ag/MoS ₂ /Au MEMRISTOR.....	16
FIGURE 13 : RC CIRCUIT FOR INTEGRATION & FIRING (R ₀ = 470 kΩ, C ₀ = 100 nF, R _L =1 kΩ).....	17
FIGURE 14: (A) VOLTAGE SCHEME WHEN APPLYING A SINGLE VOLTAGE PULSE. (B) VOLTAGE SCHEME WHEN APPLYING CONSTANT DC VOLTAGE	18
FIGURE 15: (A) SCHEMATIC ILLUSTRATION SHOWING THE CHARGING AND DISCHARGING LOOP OF NEURON CIRCUIT. (B) OUTPUT SPIKE OF THE ARTIFICIAL NEURON DEMONSTRATING THE REFRACTORY PERIOD AND INTEGRATING PERIOD.	19
FIGURE 16: (A)-(B) ARTIFICIAL NEURON SPIKING AT 3.6V. (C)-(D) ARTIFICIAL NEURON SPIKING AT 3.8V. (E) HISTOGRAM OF INTER-SPIKE INTERVAL AS A FUNCTION OF PULSE NUMBER. (F) RELATIONSHIP BETWEEN SPIKING FREQUENCY AND INPUT VOLTAGE.	20
FIGURE 17: (A) PULSE SCHEME USED. (B) CURRENT & VOLTAGE VS. TIME. (C) DISTRIBUTION OF SWITCHING TIME AT 3.5 V. (D) DISTRIBUTION OF SWITCHING TIME AT 4 V.	22
FIGURE 18: DISTRIBUTION OF TIMES IT TAKES THE Ag/MoS ₂ /Au TSM DEVICE TO SWITCH WHEN APPLYING A CONSTANT VOLTAGE OF 1 V FOR 20 SECONDS.....	23

PART 1: INTRODUCTION

1.1 NEUROMORPHIC COMPUTING

Electronic devices, such as Amazon's Alexa can perform pattern recognition by connecting to remote servers that are made up of complex circuitry. The software used to emulate this complex behavior is composed of neurons and synapses that run on conventional complementary metal-oxide-semiconductor (CMOS) based hardware that is both bulky and power hungry. With an increasing demand to improve integrated circuit (IC) performance, energy efficiency, and cost, alternative computer architectures other than the traditional von Neumann architecture, will be needed. Interestingly, the human brain can outperform many modern processors on tasks such as data classification and pattern recognition. This complex behavior is similar to a massive parallel architecture that connects low-power elements (neurons, synapses) [1]. This has motivated researchers to develop various neuromorphic devices that are inspired by the human brain's ability to perform a variety of complex tasks while consuming only 20W of power [2]. Neuromorphic systems encompass implementations that are based on biologically-inspired artificial networks and are notable for being highly parallel and requiring low power, thus having the potential to perform complex calculations faster and more efficient compared to von Neumann architectures [3]. Therefore, neuromorphic computing has become a promising candidate to meet the demands of improving IC performance and energy efficiency.

Previous attempts in developing neuromorphic systems that exhibit the brain's connectivity of neurons and synapses, such as Intel's Loihi chip, rely on CMOS technology which greatly limits the scalability and integration of the system. Two-dimensional (2D) materials, most notably 2D

transition metal dichalcogenides, have been used to realize important synaptic behaviors such as Spike Time Dependent Plasticity (STDP) and long-term potentiation and depression (LTP and LTD). This can potentially reduce the energy consumption of neuromorphic systems and can scale down the device size compared to the traditional CMOS implementations [4]. Although much work has been done to realize synapse behavior using 2D materials, there are very few reports on artificial neurons implemented in the 2D platform [5]. Trying to emulate neuron behavior has various challenges, most notably, the neuron must follow a specific behavior model and stochastic spiking should be implemented efficiently for the system to be scalable [3]. There is also a need in understanding the limitations and reliability of the devices being used to emulate this connectivity.

1.2 BIOLOGICAL NEURON

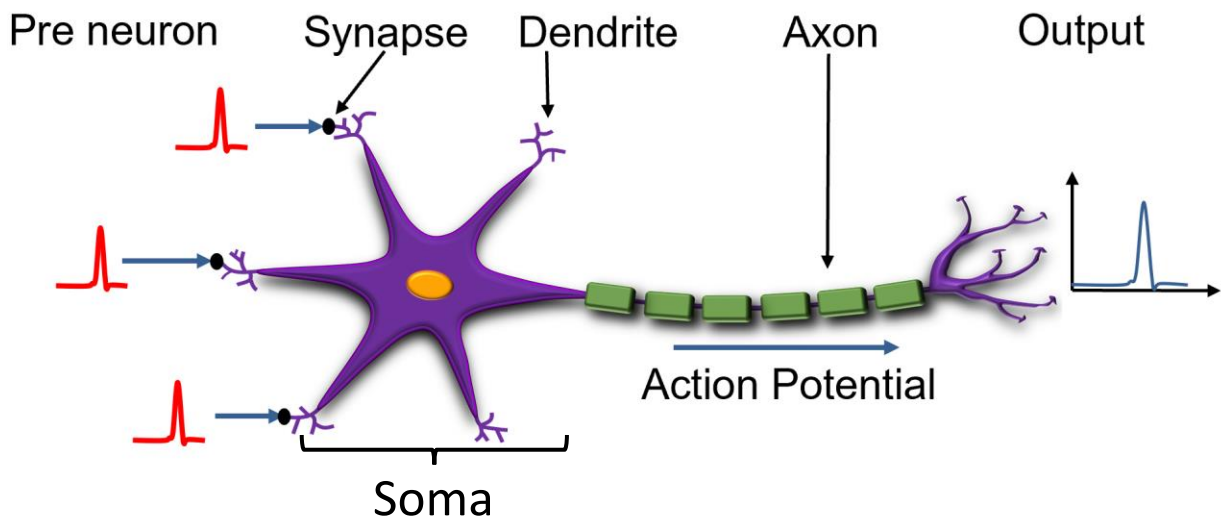


Figure 1: Representation of biological neuron [5].

In Figure 1, the soma, or cell body of the neuron, integrates the information received from the dendrites, resulting in an output, known as an action potential, if the soma's membrane potential once a certain threshold is reached. This action potential can be characterized as having a depolarization and repolarization phase (see Figure 2), followed by an undershoot phase before returning to its resting potential. Action potentials must follow two important principles:

1. All-or-nothing spiking: The neuron will either fire or not fire at all.
2. Post-refractory period: After the neuron fires, the neuron will not fire again for some duration of time, even if a signal is still be fed into the system.

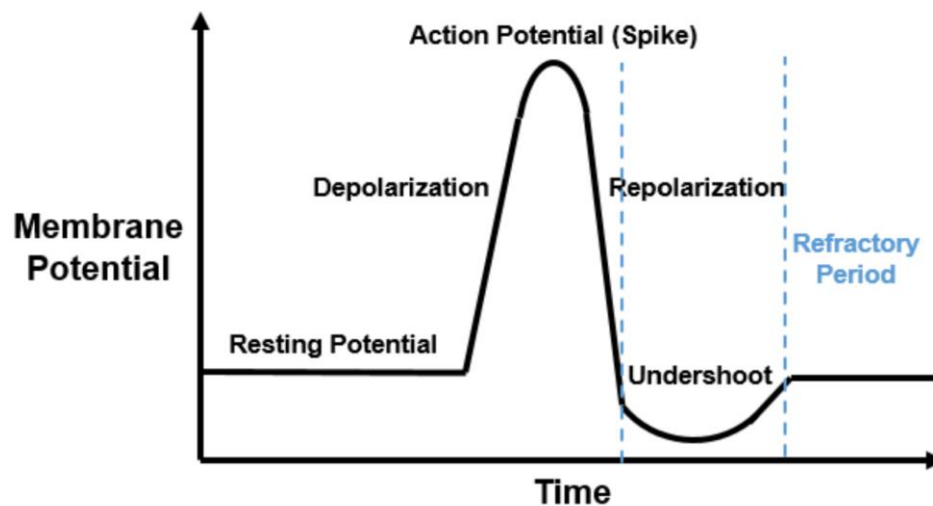


Figure 2: Features of action potential in biological neurons [6].

1.2.1 NEURON CRITICAL BEHAVIORS

The following neuron behaviors that will be emulated in this work and should be considered in neuromorphic systems:

1. All-or-nothing spiking: The neuron will either fire or not fire at all.

2. Threshold-driven firing: Once a certain threshold is met, the neuron will fire (see Figure 3).
- 3). If it is below the threshold, then the neuron will not fire at all.

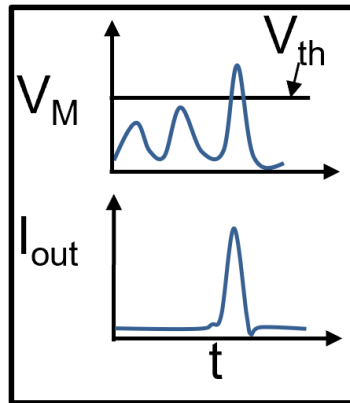


Figure 3: Simplified schematic of output spiking of neuron with respect to the input threshold [5].

3. Post firing refractory period: After the neurons fire, the neuron will not fire again for some duration of time, even if a signal is still be fed into the system. This can be further visualized in Figure 4.

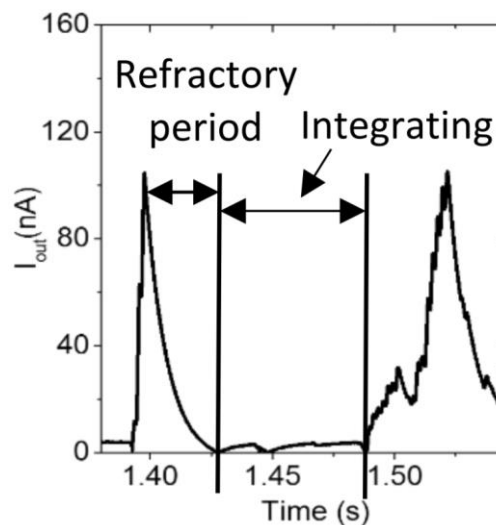


Figure 4: Output spike of artificial neuron showing the refractory and integration period of the neuron [5].

4. Stimulus strength-based frequency response: As we increase the strength of the input, the number of fires will increase. This can be seen in Figure 5, where increasing the input pulse amplitude resulted in an increase number of spikes.

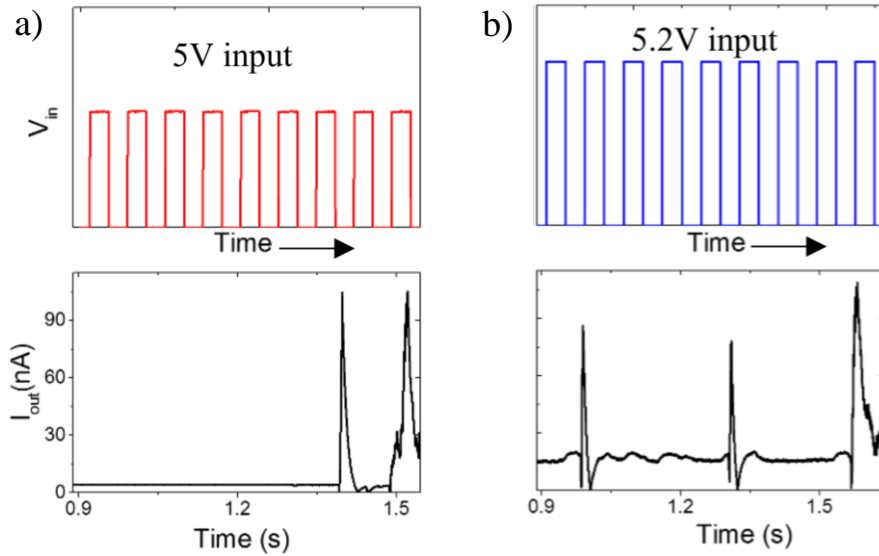


Figure 5: Stimulus strength-based frequency response for v-MoS₂/graphene TSM. (a) (Top) Input voltage pulses of amplitude 7.5V. (Bottom) Two output spike observed for input voltage pulses of amplitude 5V. (b) (Top) Input voltage pulses of amplitude 5.2 V. (Bottom) Three output spikes observed for input voltage pulses of amplitude 5.2 V [5].

1.3 THRESHOLD SWITCHING MEMRISTOR (TSM)

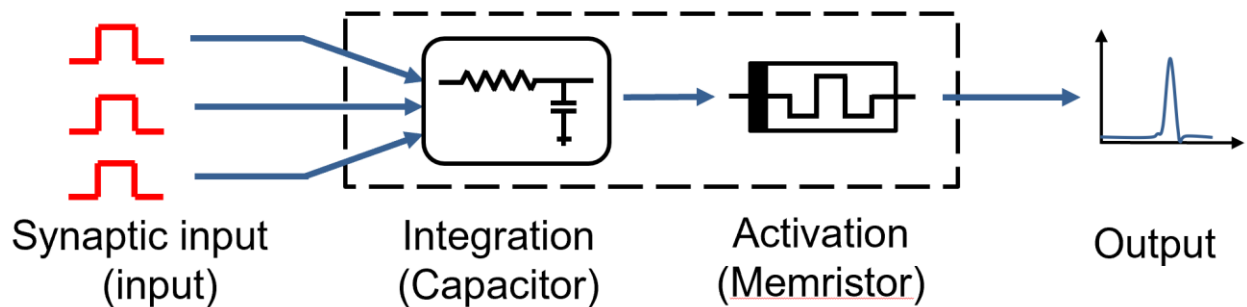


Figure 6: Conceptual representation of the TSM based artificial neuron [5].

An integrate-and-fire neuron model mimics the crucial behavior of a biological neuron that is related to the accumulation of electric charge through the soma. The capacitor integrates the charge and when the voltage across the capacitor is past the threshold value of the TSM, the neuron fires and an output spike is produced [4]. If the applied voltage is above a certain threshold (see Figure 7), the TSM device switches from a high resistance state (HRS) to the low resistance state (LRS). When the applied voltage is lower than a certain value, the device reverts to the HRS. This characteristic of TSMs are especially important in emulating the all-or-nothing and post-firing refractory period of a neuron.

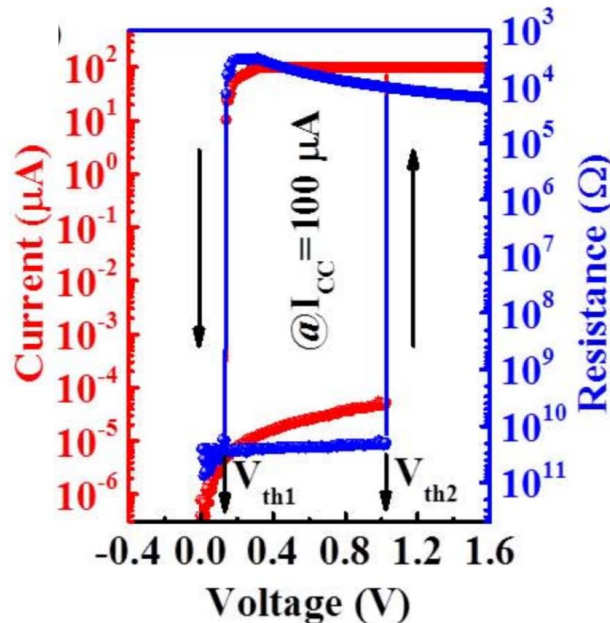


Figure 7: I-V characteristics of an Ag/SiO₂/Au TSM device [7].

1.3.1 PREVIOUS WORK EMULATING NEURON BEHAVIOR

X.Zhang et. al [7] used a Ag/SiO₂/Au threshold switching memristor to emulate the critical behaviors explained in Section 1.2.1. The TSM device was put into an RC circuit where a train of

pulses of varying amplitudes were fed into the input. It can be seen in Figure 8 that increasing the input voltage resulted in an increased number of spiking frequencies. This shows that TSM neurons are a promising candidate to be used in neuromorphic applications. More work should be done to optimize the device's operation and device's innate stochasticity should be considered.

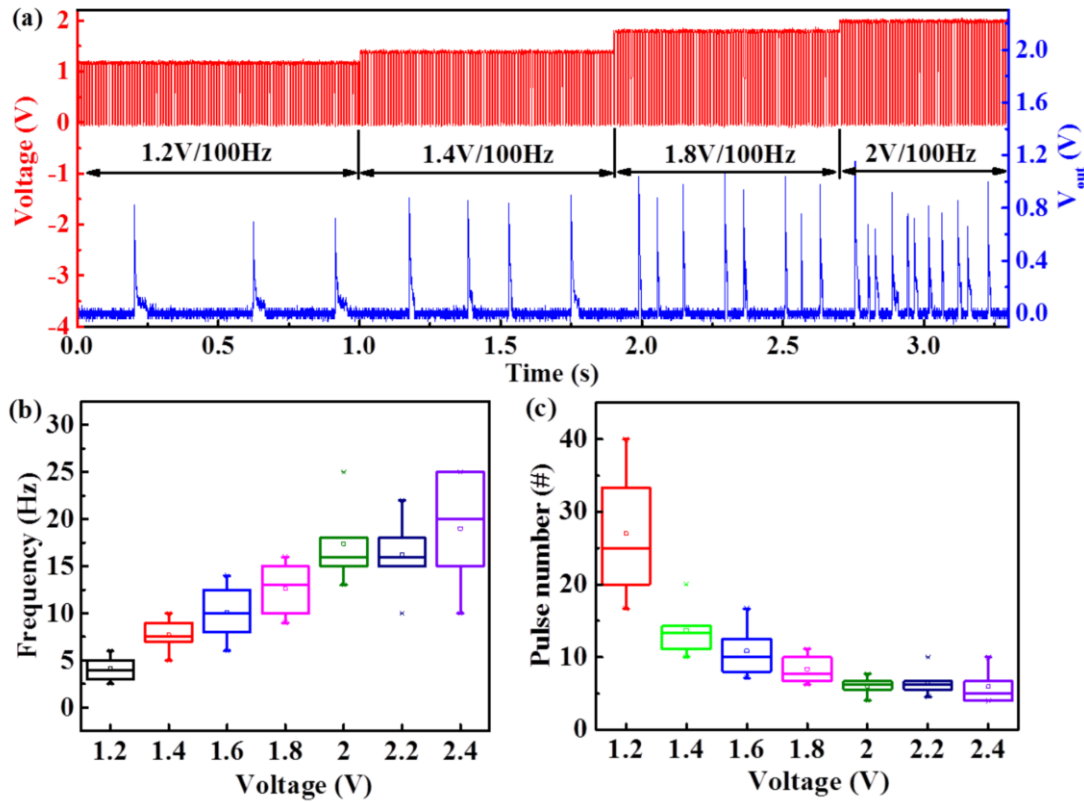


Figure 8: (a) The TSM neuron spikes under different input intensities. (b) Statistical voltage/spike-frequency relationship of the neuron. (c) The statistical pulse number/amplitude relationship of the neuron [7].

1.4 INNATE STOCHASTICITY

Although adding noise to neural networks have been found to make the system more robust and have improved performance in tasks such as data classification, not much work has been done on exploiting the innate stochasticity in memristors to realize neuron and synapse

behavior. These devices can dynamically change their resistances due to the conductive filament formation/rupture process (see Figure 9) which is intrinsically probabilistic[8]. Injecting noise into circuits comes with the cost of adding more complex CMOS circuitry, thus limiting the systems scalability. Therefore, it is becoming increasingly important to design intrinsically stochastic hardware that is both efficient and scalable[8].

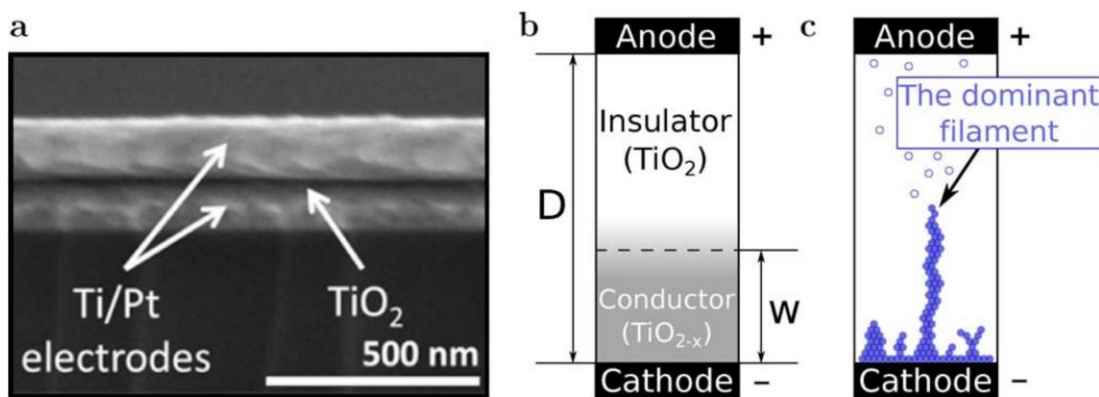


Figure 9: (a) SEM image of a TiO₂ memristor cross-section. (b) Illustration of a simple barrier memristor model. (c) Filament formation process in a thin-film [8].

1.4.1 MODELING STOCHASTIC MEMRISTORS

In the work of G. Medeiros-Ribeiro et. al, the switching time statistics for a TiO₂ memristor was measured and were found to follow a lognormal distribution. A sequence of voltage pulses was applied until the device switched at a predetermined threshold and the total time required to switch the device was recorded. This was repeated 10 times, with 10 different voltage amplitudes. The cumulative switching time probability distributions were then fit to a cumulative lognormal distribution function. S. H. Jo et. al fabricated a Ag/a-Si/p-Si pillar structure and focused on the formation of individual filaments and claimed this process was intrinsically probabilistic [10]. The wait time of the device was measured by applying a square voltage pulse and measuring the time

t , until the first sharp increase in current. The wait time distribution of different voltages was then plotted (see Figure 10). Due to the stochastic nature of the switching process, the wait time is expected to follow a Poisson distribution and the probability that a device switches within Δt is given by:

$$P(t) = \frac{\Delta t}{\tau} e^{-t/\tau}$$

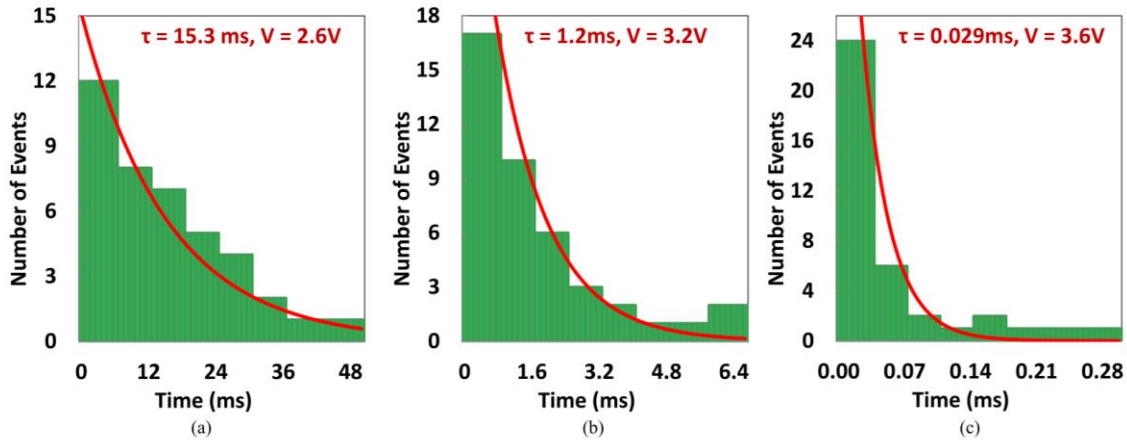


Figure 10: Histograms of the wait time for the first switching event of Ag/a-Si/p-Si pillar structure at bias voltages 2.6, 3.2, and 3.6 V, respectively [10].

This demonstrates that the wait time is highly voltage dependent. Furthermore, R. Naous, et. al using the data from [10] , the memristors were modeled and were found to have possible applications in neuromorphic circuits, most notably, the Integrate and Fire neuron, due to its innate stochasticity. This could be utilized as an alternative to noise injection in circuits where noise is beneficial.

PART 2: METHODOLOGY

The following sections depicts the structure of the Ag/2D-MoS₂/Au memristor device and how the device will be tested to see if it displays the four crucial features of neuron – all-or-nothing spiking, threshold-driven firing, post firing refractory period and stimulus strength-based frequency response.

2.1 DEVICE STRUCTURE

On a Si/SiO₂ substrate, Ti/Au (5/100 nm) bottom electrodes are patterned and deposited by e-beam evaporation. 10 nm Mo is patterned and deposited on the bottom electrodes, followed by sulfurization of the Mo to MoS₂ by chemical vapor deposition (CVD). 15 nm Ag is deposited as top electrode, and capped with 40 nm of Au. In Figure 11, a schematic of the device structure can be seen and in Figure 12, an optical image of the device can be seen.

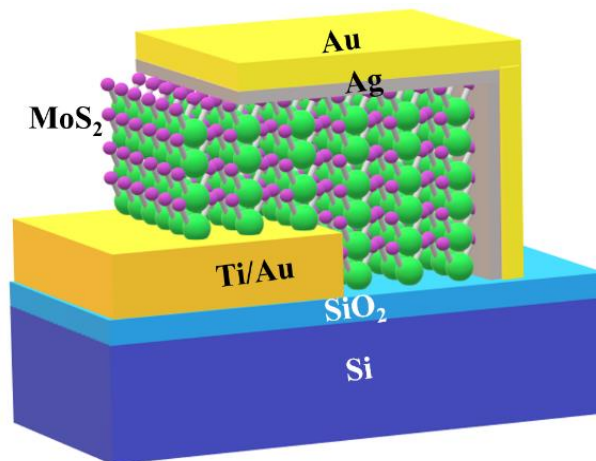


Figure 11: Structure of Ag/MoS₂/Au memristor

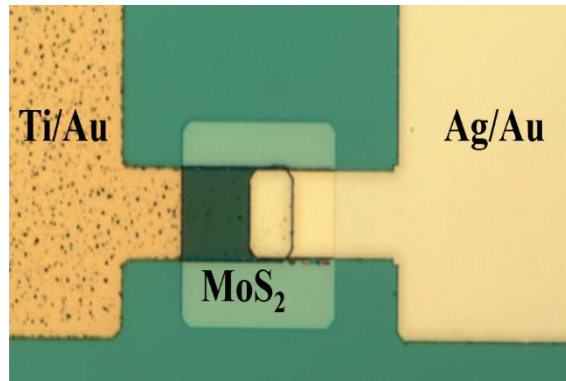


Figure 12: Optical image of Ag/MoS₂/Au memristor.

2.2 ARTIFICIAL NEURON SPIKING

In a biological neuron, upon receiving excitatory and inhibitory postsynaptic potentials, membrane potential of the neuron builds up and generates an action potential once the threshold is met. To demonstrate this, our TSM device is connected in series with an RC circuit shown in Figure 13. Long continuous train of pulses of 100 μ s are fed to the input terminal A. The TSM is initially in the high resistance state (HRS) and allows little leakage current through itself and the load resistor (R_L). The capacitor (C_o) accumulates charge and builds up potential at node B. Once the voltage at node B exceeds V_{th} , the TSM switches from HRS to low resistance state (LRS). The capacitor then discharges and the TSM generates a firing spike. This was repeated with different input voltages and a histogram of inter-spike interval as a function of pulse number was plotted and the relationship between spiking frequency and voltage pulse was found.

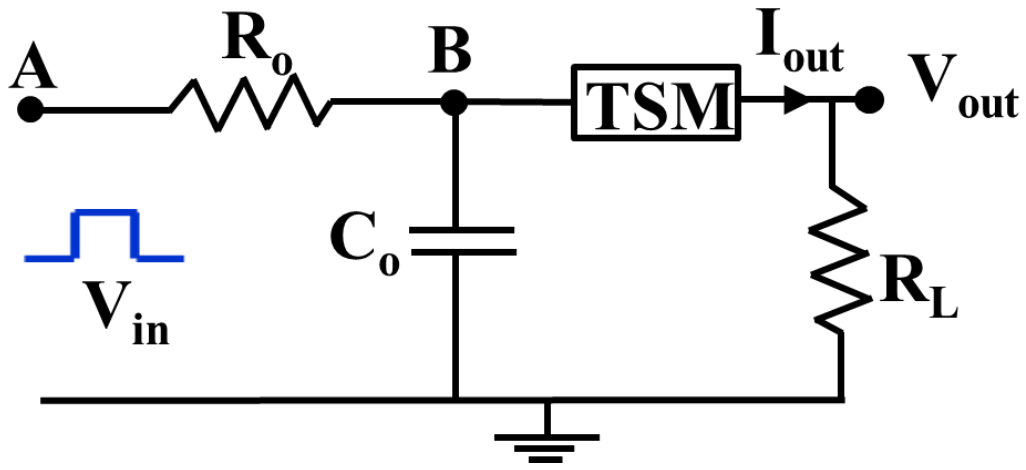


Figure 13 : RC circuit for integration & firing ($R_0= 470 \text{ k}\Omega$, $C_0= 100 \text{ nF}$, $R_L=1 \text{ k}\Omega$)

2.3 STOCHASTIC MEASUREMENTS

This measurement was conducted using a RT probe station. A single 10-millisecond pulse at a set voltage was applied to the device (see Figure 14). Since these devices are volatile, they do not need to be reset. This measurement was repeated at the same set voltage for multiple trials and the distribution of the wait time it took for the device to set was plotted. Different set voltages were also tested using the same procedure. A constant DC voltage, seen in Figure 15, for 20 seconds was applied multiple times and time it took for the device to set was plotted.

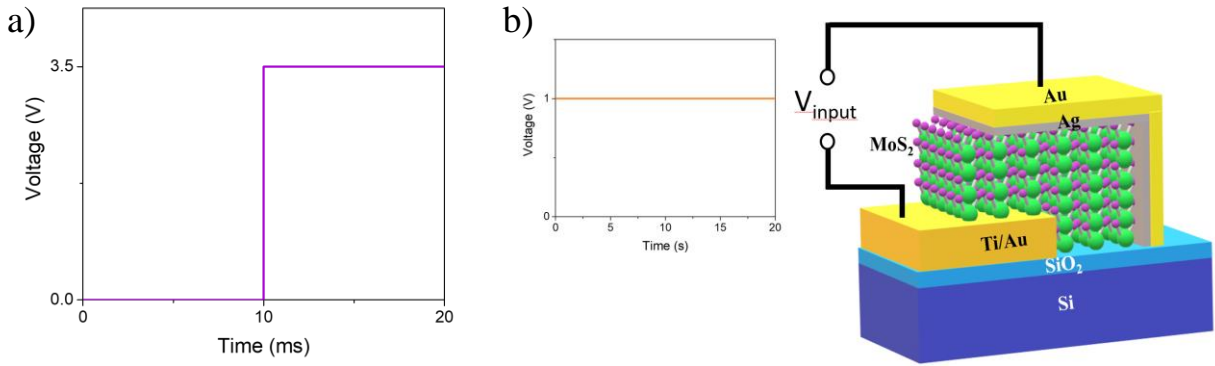


Figure 14: (a) Voltage scheme when applying a single voltage pulse. (b) Voltage scheme when applying constant DC voltage

PART 3: RESULTS

3.1 EMULATING NEURON BEHAVIOR

We have applied input pulses of varying pulse amplitude to study their impact on spiking frequency of our artificial neuron. During the refractory period, the capacitor discharges in the loop in Figure 16a. In the integration period, the capacitor is charging to get ready for the next fire, which can be visualized in the charging loop in Figure 16a. From the output current of the Ag/MoS₂/Au neuron, we can see the refractory and integration period for a 3.8 V input pulse in Figure 16b. This demonstrates the all-or-nothing and post refractory behavior of a biological neuron.

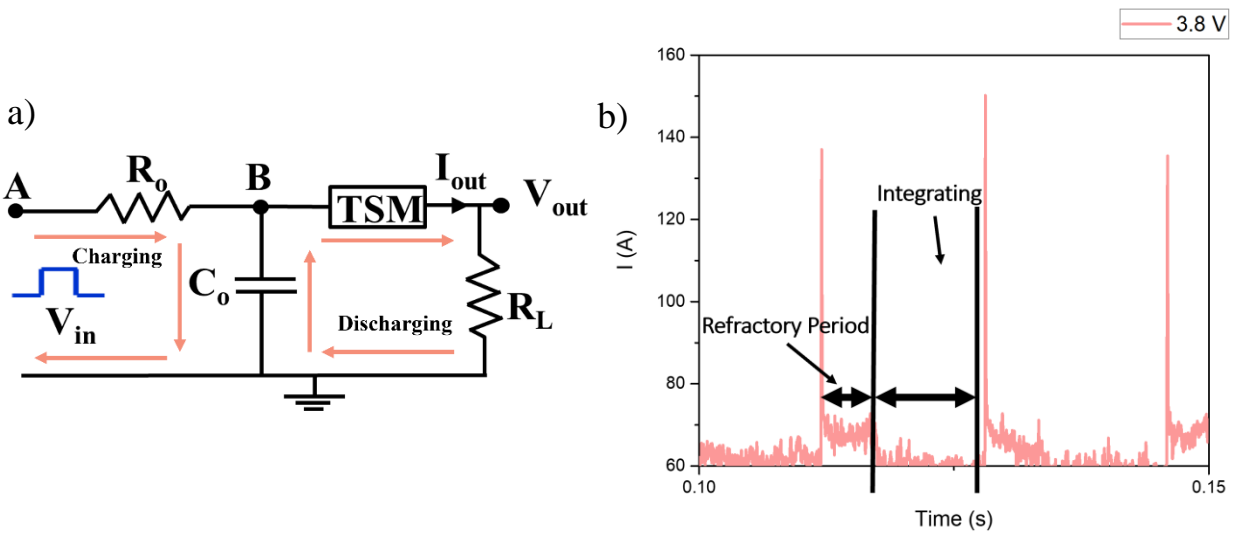


Figure 15: (a) Schematic illustration showing the charging and discharging loop of neuron circuit. (b) Output spike of the artificial neuron demonstrating the refractory period and integrating period.

Long continuous train of pulses of $100\ \mu\text{s}$ are fed to the input terminal A with amplitudes 3.6V and 3.8V (see Figure 17a and Figure 17c, respectively).

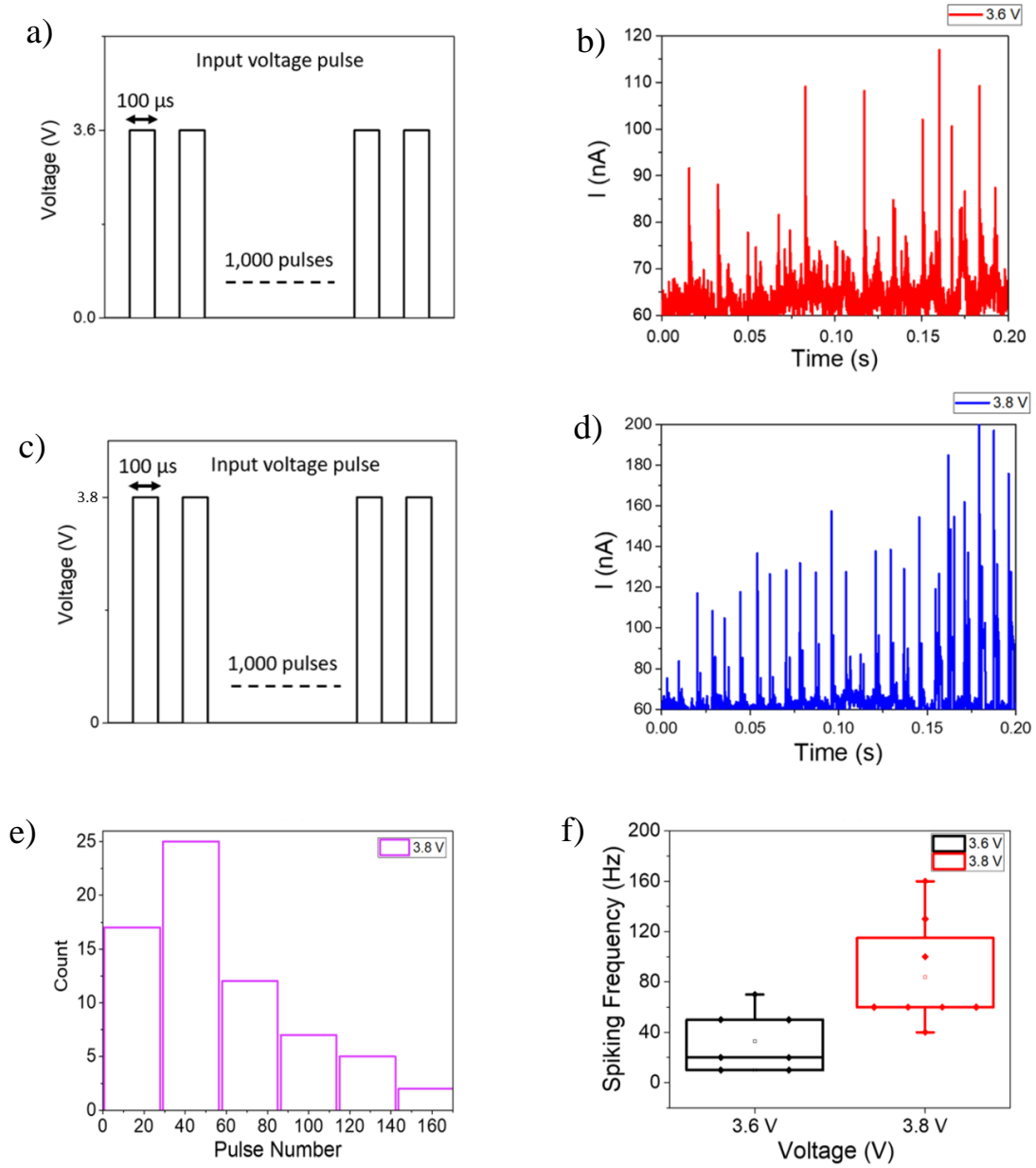


Figure 16: (a)-(b) artificial neuron spiking at 3.6V . (c)-(d) Artificial neuron spiking at 3.8V . (e) Histogram of inter-spike interval as a function of pulse number. (f) Relationship between spiking frequency and input voltage.

In Figure 17b and Figure 17d, we can see the TSM neuron spikes under different voltage amplitudes. The probabilistic distribution of pulse numbers between successful firing spikes shown in Figure 17e follows a Poisson distribution and imitates the stochastic nature of a biological neuron [12]. We observed that as we apply a higher voltage, we get an increasing number of spikes, which demonstrates the stimulus strength-based frequency response of a neuron. This relationship between spiking frequency and input voltage can be seen in Figure 17f.

3.2 STATISTICS OF DEVICE SPIKING BEHAVIOR

A 10 ms voltage pulse, which can be seen in Figure 18a, was applied to the device to find the stochastic switching behavior. If the current reached the compliance of 1 μA within the voltage pulse (see Figure 18b), the wait time was found. The wait time (Δt) is the time it takes for the device to set within the voltage pulse and was found by subtracting the time the voltage pulse is applied. It can be seen in Figure 18c and Figure 18d that the wait times follow a probabilistic distribution and that as we increase the voltage, the distribution shifts to the left, showing the decrease in average wait time.

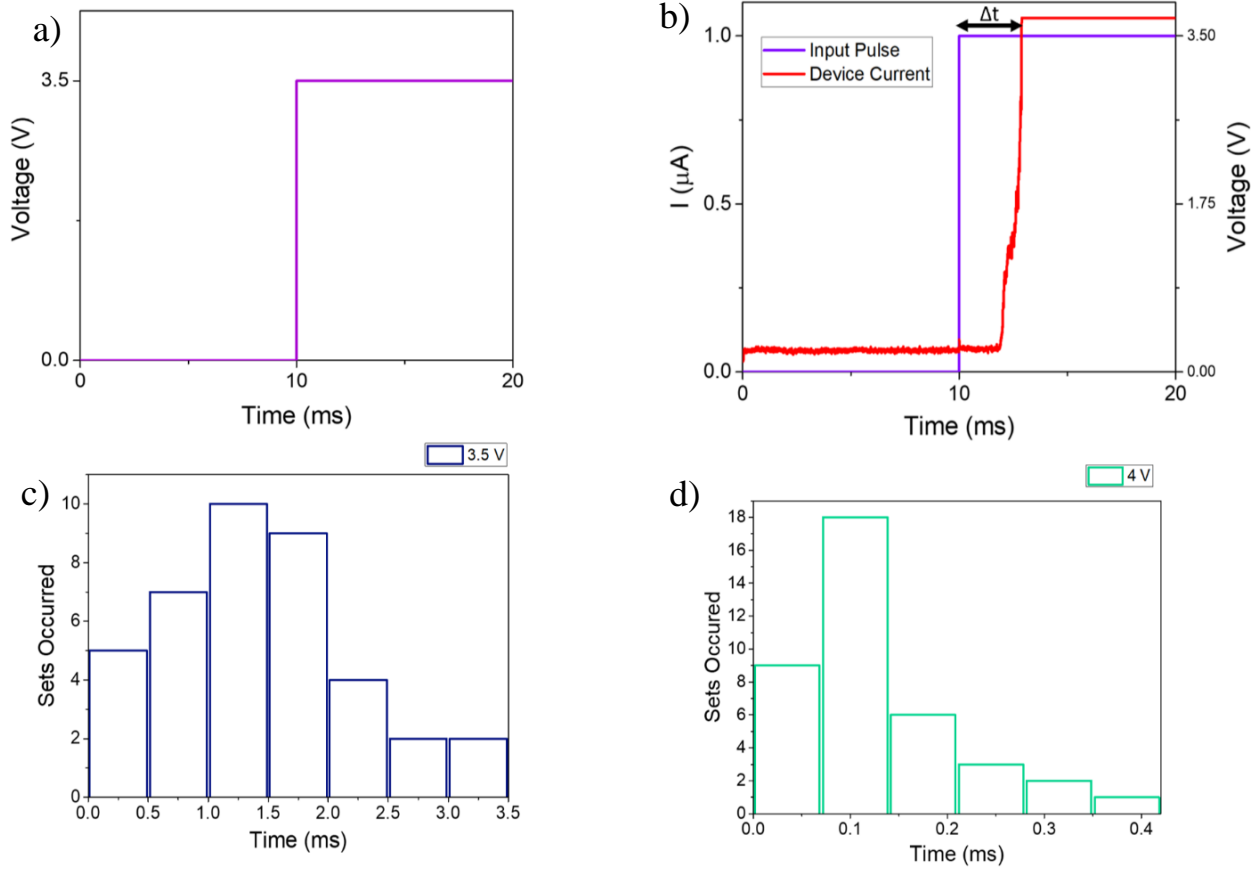


Figure 17: (a) Pulse scheme used. (b) Current & Voltage vs. Time. (c) Distribution of switching time at 3.5 V. (d) Distribution of switching time at 4 V.

A constant DC voltage of 1 V was then applied to the device for 20 seconds to see the time it takes for the device to set. In Figure 19, we can see that the switching time is stochastic when applying a DC voltage to the device.

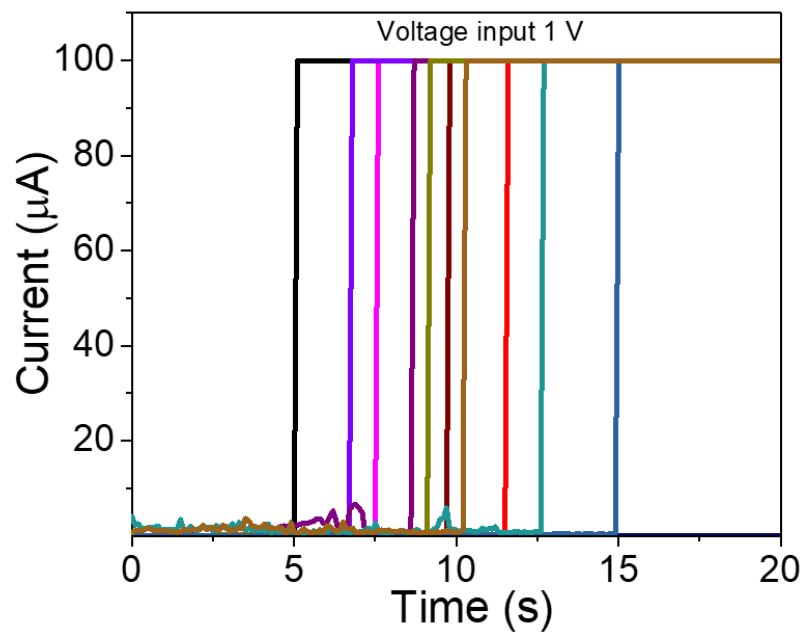


Figure 18: Distribution of times it takes the Ag/MoS₂/Au TSM device to switch when applying a constant voltage of 1 V for 20 seconds.

PART 4: CONCLUSION

In summary, we have demonstrated an Ag/MoS₂/Au threshold switching memristor based artificial neuron that emulates all four critical behaviors of a biological neuron - all-or-nothing spiking, threshold-driven firing, post firing refractory period and stimulus strength-based frequency response. We found that the relationship between inter-spike interval as a function of pulse number follows a Poisson distribution, mimicking the stochastic behavior of a biological neuron. We have also found that the time it takes the device to switch within a voltage pulse follows a Poisson distribution and that the device is voltage dependent. This means that as we increased the voltage, the wait time, or time it took the device to set decreased with increasing voltage. These results show the ability of emulating a biological neuron makes this threshold switching memristor a potential candidate for future neuromorphic computing. The device's innate stochasticity can also be utilized, most notably, in the Integrate and Fire neuron, and can be an alternative to adding complicated CMOS circuitry to inject noise in circuits where noise is beneficial.

REFERENCES

- [1] G. W. Burr *et al.*, “Advances in Physics : X Neuromorphic computing using non-volatile memory,” *Adv. Phys. X*, vol. 6149, pp. 1–21, 2017.
- [2] G. J. Siegel, B. W. Agranoff, and R. W. Albers, Eds., *Basic Neurochemistry: Molecular, Cellular and Medical Aspects*. Philadelphia, PA: Lippincott-Raven, 1999.
- [3] C. D. Schuman *et al.*, “A Survey of Neuromorphic Computing and Neural Networks in Hardware,” pp. 1–88, 2017.
- [4] S. Wang, D. W. Zhang, and P. Zhou, “Two-dimensional materials for synaptic electronics and neuromorphic systems,” *Sci. Bull.*, vol. 64, no. 15, pp. 1056–1066, 2019.
- [5] H. Kalita *et al.*, *Sci. Rep.*, vol. 9, p. 53, (2019).
- [6] Hodgkin A.L., and A.F. Huxley, “Action potentials recorded from inside a nerve fibre,” *Nature* 144, 710–711, 1939.
- [7] X. Zhang, W. Wang, Q. Liu, X. Zhao, J. Wei, and R. Cao, “An Artificial Neuron Based on a Threshold Switching Memristor,” *IEEE Electron Device Lett.*, vol. 39, no. 2, pp. 308–311, 2018.
- [8] M. Al-shedivat, S. Member, R. Naous, and G. Cauwenberghs, “Memristors Empower Spiking Neurons With Stochasticity,” *IEEE J. Emerg. Sel. Top. Circuits Syst.*, vol. 5, no. 2, pp. 242–253, 2015.
- [9] G. Medeiros-Ribeiro, F. Perner, R. Carter, H. Abdalla, M. D. Pickett, and R. S. Williams, “Lognormal switching times for titanium dioxide bipolar memristors: Origin and resolution,” *Nanotechnology*, vol. 22, no. 9, 2011.
- [10] S. H. Jo, K.-H. Kim, and W. Lu, “Programmable Resistance Switching in Nanoscale Two-Terminal Devices,” *Nano Lett.*, vol. 9, no. 1, pp. 496–500, 2009.
- [11] R. Naous, M. Al-Shedivat, and K. N. Salama, “Stochasticity modeling in memristors,” *IEEE Trans. Nanotechnol.*, vol. 15, no. 1, pp. 15–28, 2016.
- [12] Müller B., Reinhardt J., Strickland M.T. (1995) Stochastic Neurons. In: Neural Networks. Physics of Neural Networks. Springer, Berlin, Heidelberg